Journal of Solid State Chemistry **151,** 122–129 (2000)
doi:10.1006/jssc.2000.8634, available online at http://www.idealibrary.com on IDEAL®

Synthesis and Structure of $Na_2[(HO_3PCH_2)_3NH]1.5H_2O$: The First Alkaline Triphosphonate

H. Silvia Martínez-Tapia,* Aurelio Cabeza,* Sebastián Bruque,* Pilar Pertierra,† Santiago García-Granda,† and Miguel A. G. Aranda*,[1]

*Departamento de Química Inorgánica, Cristalografía y Mineralogía, Universidad de Málaga, 29071 Málaga, Spain; and
†Departamento de Química Física y Analítica, Facultad de Química, Universidad de Oviedo, 33006 Oviedo, Spain

Received October 28, 1999; in revised form December 27, 1999; accepted January 20, 2000

Sodium nitrilotris(methylenephosphonate), $Na_2[(HO_3PCH_2)_3NH]1.5H_2O$, has been synthesized as single crystals and as bulk polycrystalline single phase. This compound is triclinic, space group $P\bar{1}$, $a = 7.398(1)$ Å, $b = 8.446(1)$ Å, $c = 10.086(1)$ Å, $\alpha = 81.39(1)^\circ$, $\beta = 89.29(1)^\circ$, $\gamma = 81.18(1)^\circ$, $Z = 2$ and the structure was solved from single-crystal data. The crystal structure was used to refine the powder diffraction data by the Rietveld method. The structure contains Na_4O_{16} tetramers, with the sodiums cations in distorted oxygen octahedral environments, and molecular units of the acid triphosphonate with protonated nitrogen atom. The framework is three-dimensional with small channels where two types of water molecules are located. This material has also been characterized by thermal analysis, including a thermodiffractometric study, and infrared spectroscopy. © 2000 Academic Press

Key Words: **soluble metal phosphonates; hybrid organo-inorganic composites.**

INTRODUCTION

Metal phosphonate chemistry has attracted a lot of interest in the past two decades (1–3). A main reason for the growth of research in metal organo-phosphonates is the wide variety of structures that these materials can present: one-dimensional chains, layered structures, and three-dimensional microporous frameworks (1). Furthermore, a very attractive feature is that they allow us to have a certain control over the dimensionality of the metal phosphonates by the suitable choice of the phosphonic acid used in the synthesis. So, pillared layered phosphonates (PLSs) can be synthesised by using, for example, diphosphonic acids H_2O_3P–*R*–PO_3H_2 as pillaring agent (4), or by the choice of the functional end *Z* of the phosphonic acid, H_2O_3P–*R*–*Z* ($Z = CO_2H$, NH_2) (5). The use of functionalized phosphonic acids allows us to study not only how the functionalized end may dictate the dimensionality of the solid, but also the reactivity that these organic functions may show. Consequently, these materials can find a great number of practical applications as catalysts, hosts in intercalation compounds, sorbents, ion exchangers, protonic conductors, and components in the preparation of films possessing optical, nonlinear optical, or electronic properties (6).

Although the main research effort in the metal phosphonates field was initially directed toward tetravalent cation phosphonates (for instance Zr, Ti, Sn, Ce), many other works have been reported about the synthesis, crystal structures, and properties of divalent, trivalent, and even pentavalent metal phosphonates. However, very little research has been carried out on monovalent phosphonates. In fact, to the best of our knowledge, no alkaline phosphonate has been reported so far. There are reports of phosphonates containing alkaline cations but in addition to other transition metals, like in $Cs[VO(HO_3P–CH_2–PO_3)]$ (7).

We have recently reported the preparation and structures of two divalent lead-functionalized triphosphonates, $Pb[(HO_3PCH_2)_3NH]$ and $Pb_2[(O_3PCH_2)_2NH(CH_2PO_3H)]\cdot H_2O$ (8). As part of our research effort in functionalized phosphonates, in this paper, we describe the synthesis and characterization of the first alkaline triphosphonate, $Na_2[(HO_3PCH_2)_3NH]1.5H_2O$.

EXPERIMENTAL

The tested sources of nitrilotris(methylene)triphosphonic acid (TPA) were 50 wt% solution from Aldrich (Aldrich-TPA) and 97 wt% pure solid from Fluka (Fluka-TPA). Solid NaOH (98%, Prolabo) was used as a source of sodium and to regulate the pH. These reactants were used without purification.

Elemental analysis. Carbon, nitrogen, and hydrogen contents were determined by elemental chemical analysis on

[1] To whom correspondence should be addressed. Fax: Int-34-952132000. E-mail: g_aranda@uma.es.

0022-4596/00 $35.00

a Perkin-Elmer 240 analyzer. Na content was determined by atomic emission spectroscopy in a Perkin-Elmer 3100 spectrophotometer.

Thermal analysis. TGA and DTA data were collected on a Rigaku Thermoflex apparatus at heating rate 10 K min^{-1} in air with calcined Al_2O_3 as internal reference standard in air.

Infrared study. Infrared spectra were recorded on a Perkin Elmer 883 spectrometer in the spectral range 4000–200 cm^{-1}, by using dry KBr pellets containing 2% of the sample.

X-Ray powder diffraction. Room temperature X-ray powder diffraction patterns were collected on a Siemens D-5000 automated diffractometer using graphite-monochromated Cu$K\alpha$ radiation. The powder thermodiffractometric study was carried out in air with the same diffractometer but in a second goniometer permanently equipped with an HTK10 heating chamber. The samples were packed over the Pt foil that is both the heating system and the holder. The thermodiffractometric patterns were scanned over the angular range 6–30° (2θ), with a step size of 0.04° and counting for 5 s per step. The appropriate heating and cooling temperatures were selected by using the Diffract AT software. The samples were held at each temperature for 10 min, before recording of any pattern, to ensure that any transformations that may take place were allowed time to do so. The powder patterns of the sample display a strong preferred orientation that was minimized prior to data collection as explained latter.

X-ray crystallographic procedures. A colorless crystal was mounted in a Nonius CAD4 single-crystal diffractometer. Unit cell dimensions were determined from the angular settings of 25 reflections with $10 < \theta < 15°$. Some data collection details are given in Table 1. A total of 2562 reflections were measured by using the ω–2θ scan technique with a variable scan rate and a maximum counting time of 60 s per reflection. Intensity was checked throughout the data collection by monitoring three standard reflections every 60 min. Final drift corrections were between 0.93 and 1.03. Profile analysis was performed on all reflections (9, 10). Some double measured reflections were averaged, $R_{int} = 0.076$, yielding 2415 unique reflections and 1597 "observed" with $I > 2\sigma(I)$. Lorentz and polarization corrections were applied and the data were reduced to F_0^2 values. The structure was solved by direct methods using the program SHELXS90 (11) and expanded with DIRDIF (12). Isotropic least-squares refinement, using SHELXL93 (13), converged to $R1 = 0.088$. Positional parameters and anisotropic thermal parameters of the nonhydrogen atoms were refined on F^2. All hydrogen atoms were isotropically refined with a common thermal parameter. Because of the compositional disorder found, the O–H bonds of the water molecules needed the use of geometrical restraints. The final conventional agreement factors and pertinent crystallographic details are given in Table 1. The maximum shift over the error ratio in the last full-matrix least-squares cycle was less than 0.020. Atomic scattering factors were taken from the *International Tables of X-ray Crystallography* (14). Geometrical calculations were made with PARST (15). All single-crystal data calculations were made at the University of Oviedo on the Scientific Computer Center and X-ray Group AXP computers.

TABLE 1
Single-Crystal Crystallographic Data for $Na_2[(HO_3PCH_2)_3NH]1.5H_2O$

Empirical formula	$Na_2NP_3O_{10.5}C_3H_{13}$
Formula mass/g mol^{-1}	370.03
Dimensions/mm	$0.13 \times 0.10 \times 0.07$
Temperature/K	200(2)
Wavelength/Å	0.71073
Space group	$P\bar{1}$
a/Å	7.3982(14)
b/Å	8.4457(12)
c/Å	10.0864(12)
α/°	81.394(12)
β/°	89.285(11)
γ/°	81.179(11)
V/Å^3	615.73(16)
Z	2
D_c/g cm^{-3}	1.996
μ/mm^{-1}	0.606
$F(000)$	378
θ range for data collection (°)	2.04–26.03
Index ranges	$-9 \le h \le 9$, $-10 \le k \le 10$, $0 \le l \le 12$
Reflections collected	2562
Independent reflections	2415 [R(int) = 0.076]
Refinement method	Full-matrix least-squares on F^2
Data/parameters/restraints (Å)	2415/214/5
	O(W1)–H(W1) 0.95(5)
	O(W1)–H(W2) 0.95(5)
	H(W1)–H(W2) 1.55(5)
	O(W2)–H(W3) 0.95(5)
	O(W2)–H(W4) 0.95(5)
Goodness-of-fit on F^2, χ	1.005
R indices [$I > 2\sigma(I)$]	$R1 = 0.071$, w$R2 = 0.196$
R indices [all data]	$R1 = 0.118$, w$R2 = 0.237$
Largest diff. peak and hole	1.05 and -1.13 e Å^{-3}

Synthesis of $Na_2[(HO_3PCH_2)_3NH]nH_2O$ ($1.5 < n < 2$), Na-TPA

(**I**) Na-TPA was prepared as a polycrystalline solid by addition of 4.23 g of NaOH to 24.3 ml of a solution of Aldrich TPA at room temperature. Under these conditions the pH was 1.68 and a white solid started to appear. Then, the mixture was refluxed for 8 days and the resulting white

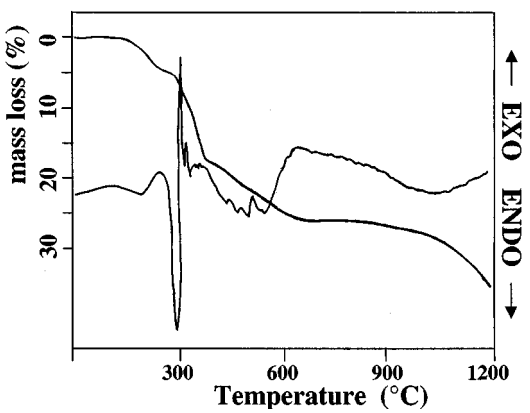

FIG. 1. TGA–DTA curves for $Na_2[(HO_3PCH_2)_3NH]1.5H_2O$.

solid was filtered off, washed with distilled water at ~0°C, and dried at 60°C.

(**II**) Polycrystalline Na-TPA was also prepared from Fluka TPA. First, a solution of 2.3544 g of solid TPA in 6 ml of water was prepared. Then, 0.8444 g of NaOH was slowly added to the former solution which resulted in a suspension of pH 2.08. This mixture was refluxed for 1 day and the resulting white solid was treated as in method **I**.

(**III**) Single crystals of Na-TPA were prepared hydrothermally as follows: 24.3 ml of a solution of Aldrich TPA was diluted with 3 ml of H_2O. Then, 4.23 g of NaOH was added which resulted in the starting of the precipitation of the white solid. This saturated mixture was hydrothermally heated in a Teflon-lined autoclave at 130°C for 4 days, and cooled to room temperature slowly over 3 days. A solution with small transparent crystals was obtained in this way. The crystals were treated as in method **I** but dried at 40°C.

Analytical data: Na, 13.7%; C, 9.90%; N, 3.36%; H, 3.73%. Calculated data for $Na_2[(HO_3PCH_2)_3NH]1.5H_2O$: Na, 12.43%; C, 9.72%; N, 3.51%; H, 3.78%.

RESULTS AND DISCUSSION

We have described here three of our several synthetic ways to obtain single-phase Na-TPA. Aldrich-TPA is much cheaper than Fluka-TPA but the solution contains many impurities like less substituted phosphonic acids (e.g., $(H_2O_3PCH_2)_2NH$), and other acids like phosphoric and hydrochloric. So, we have conducted tests to verify that the preparations from both starting materials lead to the same solid. In any case, the precipitation of Na-TPA starts at quite low values of pH (< 2.0), suggesting that the solid has many protons in the structure as was verified by IR and structural studies. It is worth emphasizing that this sodium phosphonate is very soluble and can be used as a starting compound for the synthesis of metal phosphonates when low pH's are undesirable. The attempts to grow single crystals at room temperature by slow addition, diffusion, and crystallization from solution were unsuccessful. The resulting crystals under these conditions presented many defects and very small sizes. Good crystals could be ob-

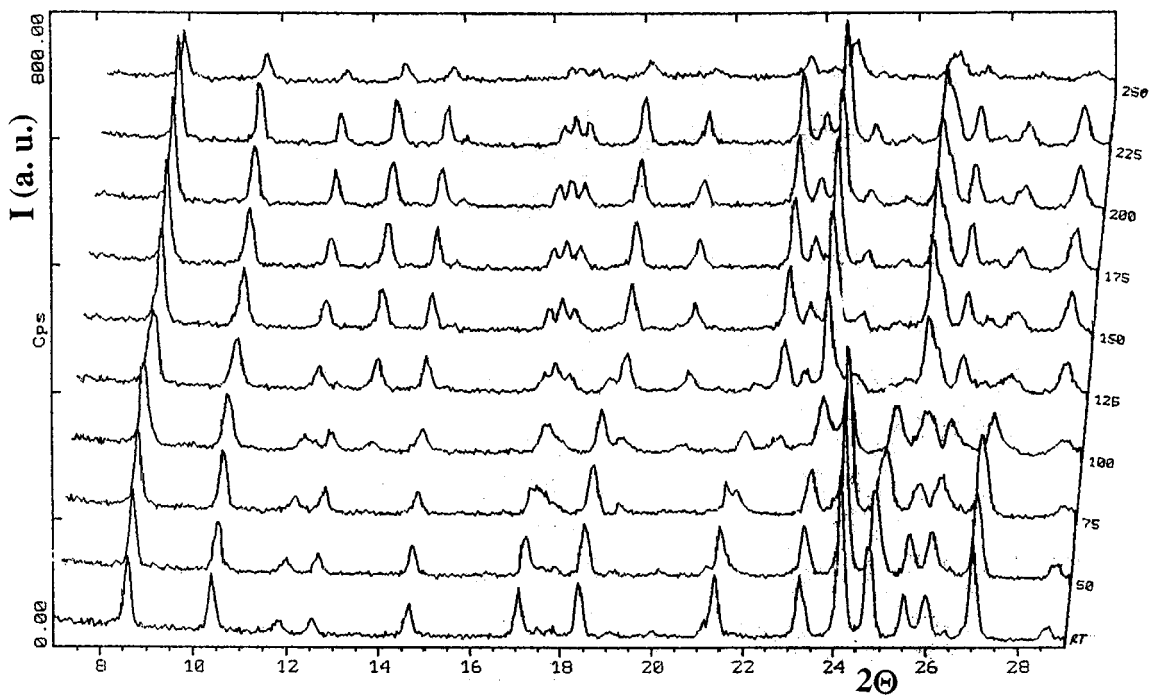

FIG. 2. X-ray thermodiffractometric patterns for $Na_2[(HO_3PCH_2)_3NH]1.5H_2O$.

tained only at higher temperatures by using hydrothermal conditions and with slow cooling rates.

Thermal Study

TGA-DTA curves for $Na_2[(HO_3PCH_2)_3NH]1.5H_2O$ (**III**) are shown in Fig. 1. The DTA curve shows several endothermic effects and one exothermic effect. The sharp exothermic effect observed at 300°C is due to the combustion of the organic nitrogenated fraction of the sample with the release of NO_x, CO_2, and H_2O gases. The first broad endothermic effect is centered below 200°C and it is due to the loss of part of the hydration water (approximately 0.5 water molecule per chemical formula). The second sharp endotherm is also due to the water loss although these losses are overlapped and it is difficult to determine the exact amount of water loss of each step. Furthermore, different syntheses at room temperature led to compounds with similar X-ray powder patterns but slightly different water contents although never higher than 2 water molecules per chemical formula. A set of weak endotherms are located between 400 and 600°C. The overall weight loss at 600°C is 24.5% and it agrees fairly well with the calculated water loss of 24.43% for the release of the volatiles leading to a residue of composition $Na_2O \cdot 1.5P_2O_5$. The powder pattern of the heating decomposition product (between 650 and 850°C) is amorphous, which is a characteristic of alkaline glassy phosphates. This solid is unstable above 900°C and a loss of P_2O_5 is observed.

A thermodiffractometric study (Fig. 2) was undertaken to characterize the water loss in the temperature range between 25 and 250°C. The first slight modification of the powder pattern is observed between 100 and 125°C (static) which is very likely due to the loss of $0.5H_2O$ molecule per chemical formula. As we will show, the structure of this compound is not layered and there is no modification in the value of the large *d*-spacing peaks. The monohydrate compound, $Na_2[(HO_3PCH_2)_3NH]H_2O$, is stable over a large temperature range up to 225°C. Above this temperature, a large modification of the powder pattern is observed which is due to the decomposition of the sample. To avoid the preferred orientation effects of the sample packed over the Pt foil we proceeded as previously reported (16). We diluted and blended the sample with spherical nanoparticles (i.e., finely ground amorphous silica gel), in this case Cab-O-Sil from Fluka. After we checked that the mixture displayed little preferred orientation, we packed this mixture over the Pt holder.

IR Spectroscopic Study

The IR spectrum of $Na_2[(HO_3PCH_2)_3NH]1.5H_2O$ was recorded between 4000 and 800 cm^{-1} and it is shown in Fig. 3. The position of the bands and the relative transmittances are given in the auxiliary material (Table 4, available from the authors). The region between 4000 and 1500 cm^{-1} can be selected to study in detail the hydration water and the protonated groups. Two bands are observed at 3630 and 3556 cm^{-1}. The first band is sharp and it is probably due to the stretching vibration of an O–H of a water molecule that it does not interact through H-bonding by the hydrogen. The second band is much broader and it is likely due to the stretching of an O–H group when the water molecule is interacting by H-bonding through the hydrogen. The presence of two water molecule types evident in the thermal study and in this spectroscopic study was confirmed by the structural study (see next section). A shoulder is observed at $\sim$3400 cm^{-1} which is probably due to the stretching vibration of the N–H group. The C–H stretching vibration is observed at 3042 cm^{-1}. Two bands are observed at 2861 and 2333 cm^{-1} and they are likely due to ν PO–H and the overtone 2δ P–O–H, respectively. These bands are typical of hydrogen phosphonates (8). The bending H–O–H vibration of the hydration water is located at $\sim$1630 cm^{-1}, as an

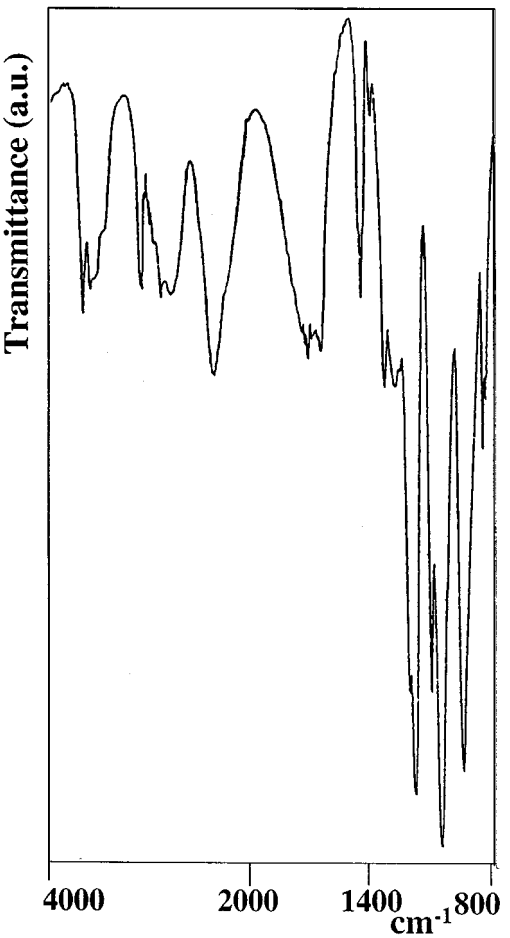

FIG. 3. IR spectrum for $Na_2[(HO_3PCH_2)_3NH]1.5H_2O$.

intense broad band. In fact, the band presents another close maximum at 1695 cm^{-1} which is usually assigned to the bending vibrations of species containing highly mobile protons, typical of good protonic conductors. Other bands typical of phosphonates are given in Table 4 (auxiliary material, available from the authors).

Structural Study

The X-ray laboratory powder pattern of $Na_2[(HO_3PCH_2)_3NH]1.5H_2O$ was autoindexed using the TREOR90 program (17) giving a triclinic unit cell with $a = 7.303(4)$ Å, $b = 8.482(7)$ Å, $c = 10.119(5)$ Å, $\alpha = 82.21(1)^\circ$, $\beta = 89.41(1)^\circ$, $\gamma = 99.25(1)^\circ$, $V = 612.8$ Å^3, $Z = 2$, V_{at} (non-H atom) = 15.32 Å^3/at, $M_{20} = 22$ (18), and $F_{20} = 45$ (0.012, 38). We tried to solve the crystal structure *ab initio* from powder diffraction data. However, although the cell volume is not very big our attempts were unsuccessful. This was mainly due to broad peaks present in the powder pattern and to the absence of heavy cations that makes the *ab inito* procedure in powder diffraction less straightforward.

Due to the high solubility of this compound and the mild conditions needed to synthesize it we came back to chemistry to grow single crystals. After some attempts, we succeeded in growing them hydrothermally as explained above. The structure was solved as indicated in the experimental part and pertinent crystallographic data are shown in Table 1. Atomic parameters are given in Table 2 and selected bond distances are given in Table 3. Hydrogen positions and anisotropic thermal parameters are given as auxiliary material in Tables 5 and 6, respectively (available from the authors).

TABLE 2
Atomic Coordinates ($\times 10^4$) and Equivalent Isotropic Displacement Parameters (Å$^2 \times 10^3$) for $Na_2[(HO_3PCH_2)_3NH]1.5H_2O$

Atom	x	y	z	U_{eq}
Na(1)	8854(3)	3264(3)	5619(2)	13(1)
Na(2)	8184(4)	5296(3)	12150(3)	17(1)
P(1)	6079(2)	7222(2)	4501(2)	8(1)
O(1)	6438(6)	8995(5)	3983(5)	14(1)
O(2)	4358(7)	6929(6)	3856(5)	17(1)
O(3)	7800(6)	6044(6)	4419(5)	14(1)
C(1)	5466(8)	7218(7)	6257(6)	8(1)
P(2)	7387(2)	4457(2)	8813(2)	12(1)
O(4)	7891(8)	3975(6)	10264(5)	22(1)
O(5)	8816(6)	4173(6)	7765(4)	14(1)
O(6)	5667(7)	3697(6)	8518(5)	22(1)
C(2)	6719(10)	6642(8)	8583(6)	14(1)
P(3)	9969(2)	8935(2)	7165(2)	9(1)
O(7)	10821(6)	7449(5)	6612(4)	12(1)
O(8)	10393(8)	8768(7)	8692(6)	29(1)
O(9)	10328(6)	10577(6)	6517(5)	18(1)
C(3)	7501(9)	9041(8)	7015(7)	11(1)
OW1	2152(9)	1897(8)	8815(6)	38(2)
OW2[a]	4610(3)	9650(2)	200(3)	79(6)
N(1)	7029(7)	7338(6)	7146(5)	8(1)

Note. U_{eq} is defined as one-third of the trace of the orthogonalized U_{ij} tensor. Refined hydrogen positions are given in auxiliary material (available from the authors).

[a]Occupation factor = 0.50.

TABLE 3
Selected Bond Lengths (Å) for $Na_2[(HO_3PCH_2)_3NH]1.5H_2O$

Na(1)–O(5)	2.401(5)	Na(2)–O(5)	2.336(5)	O(3)–H(1)	0.98(9)
Na(1)–O(9)	2.410(5)	Na(2)–O(4)	2.372(5)	O(6)–H(2)	0.89(9)
Na(1)–O(7)	2.415(5)	Na(2)–OW1	2.401(7)	O(8)–H(3)	0.84(9)
Na(1)–O(2)	2.453(5)	Na(2)–O(3)	2.466(5)	N(1)–H(4)	0.92(9)
Na(1)–O(3)	2.489(5)	Na(2)–O(7)	2.472(5)		
Na(1)–O(3)	2.628(5)	Na(2)–O(6)	2.903(6)		
P(1)–O(3)	1.501(5)	P(2)–O(4)	1.496(5)	P(3)–O(7)	1.497(5)
P(1)–O(2)	1.507(5)	P(2)–O(5)	1.504(5)	P(3)–O(9)	1.504(5)
P(1)–O(1)	1.572(5)	P(2)–O(6)	1.561(5)	P(3)–O(8)	1.557(6)
P(1)–C(1)	1.822(6)	P(2)–C(2)	1.816(7)	P(3)–C(3)	1.821(7)
C(1)–N(1)	1.497(8)	C(2)–N(1)	1.509(8)	C(3)–N(1)	1.518(8)
C(1)–H(11)	1.11(8)	C(2)–H(12)	1.05(9)	C(3)–H(13)	0.98(8)
C(1)–H(21)	1.04(8)	C(2)–H(22)	1.03(8)	C(3)–H(23)	0.91(9)

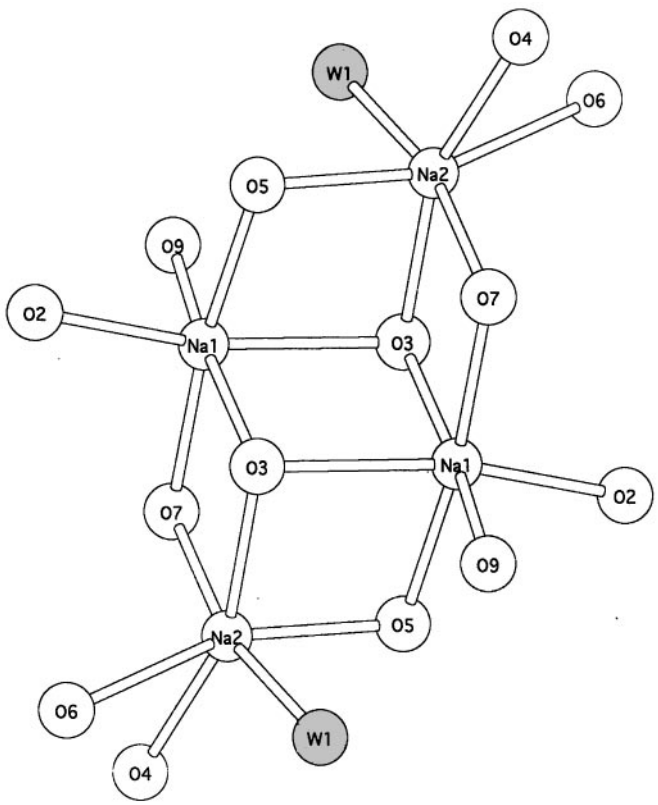

FIG. 4. Na_4O_{16} tetramer present in $Na_2[(HO_3PCH_2)_3NH]1.5H_2O$.

The crystal structure contains two types of NaO_6 octahedra (bond distances given in Table 3) which form centrosymmetric tetramers Na_4O_{16} by sharing edges as shown in Figure 4. The other structural unit is the nitrilotris (methylenephosphonic) group which displays a geometry as expected—seven tetrahedral groups: three phosphonates CPO_3, three methylenes PCH_2N, and an HNC_3 group. The hydrogen phosphonate oxygens (O1, O6, O8) present P–O bond lengths larger than those of the ionic phosphonate oxygens P–O groups as also expected. The isolated tetramers are linked by the nitrilotris(methylene)triphosphonate groups to generate a three-dimensional framework. The structure of the organic acid is similar to those found in divalent triphosphonates (8) but the inorganic coordination polyhedra are very different, which reflects the flexibility of the hybrid organo-inorganic composite materials.

One water molecule is directly bonded to Na2 (OW1) while the other water molecule, OW2, with an occupation factor 0.5, is only retained by H-bonding interactions and is located close to the center of the channel formed by the above-described framework, Fig. 5. The loss of this second water molecule is observed in the thermodiffractometric study at 125°C and when it is released, it causes little modification in the structure as evidenced in the thermodiffractometric study. However, when the OW1 is lost, the structure collapses as it is necessary to satisfy the coordination requirements of the sodium cations.

The small channels with the water molecules and the presence of many protons of the hydrogen phosphonate groups make this structure suitable for an ionic conductivity study to check for possible proton ionic conductivity. Furthermore, the strong IR band centered approximately at $1700\ cm^{-1}$ also suggests mobile protons which could lead to proton conductivity. Unfortunately, it is very difficult to make a good pellet of this compound as it cannot be heated. Preliminary ionic conductivity studies in a low-quality pellet suggest very small conductivity. However, an ionic conductivity study in a large single crystal is planned to properly assess the protonic conductivity of this material.

Finally, a powder diffraction Rietveld study (19, 20) of the room temperature Na-TPA powders was carried out to verify that the structure is similar to that determined from a single crystal of hydrothermally synthesized Na-TPA. This was done as some small deviations in the unit cells were observed in the samples. To avoid/minimize the strong preferred orientation observed along the *c*-axis, the powder pattern was collected in a sample disordered in the tubular aerosol suspension chamber (TASC) as previously reported

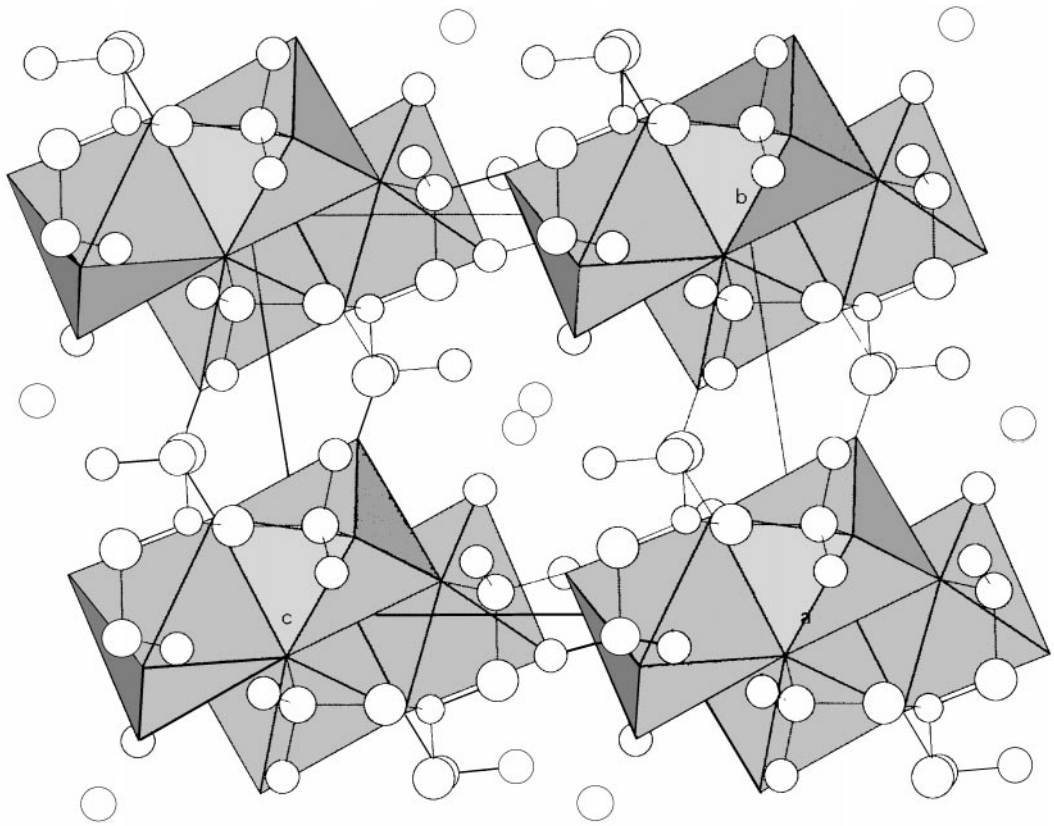

FIG. 5. [1 0 0] View of the crystal structure of $Na_2[(HO_3PCH_2)_3NH]1.5H_2O$ with Na_4O_{16} polyhedra.

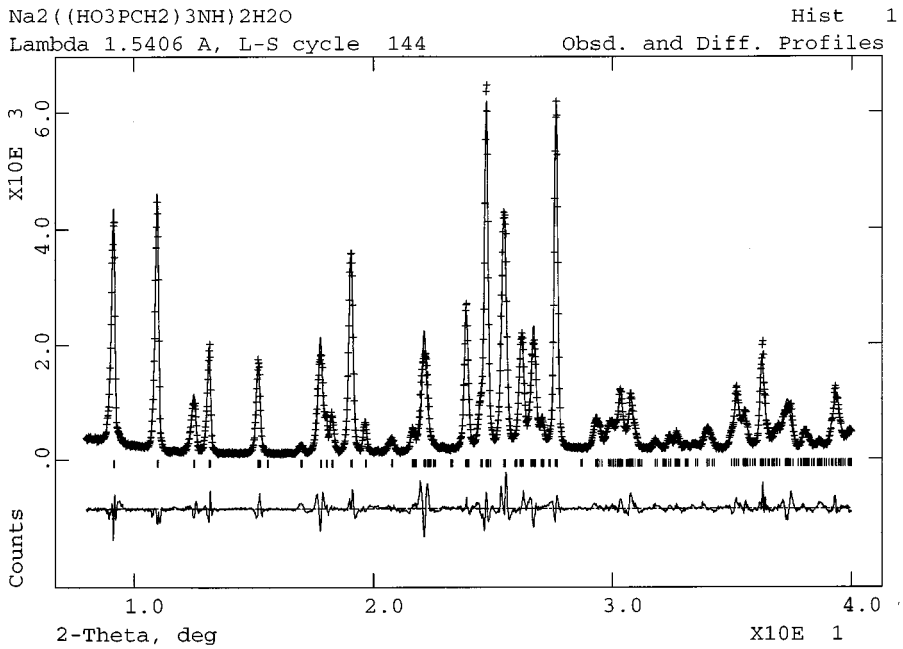

FIG. 6. Observed, calculated, and difference X-ray powder diffraction profiles for $Na_2[(HO_3PCH_2)_3NH]1.5H_2O$. The tic marks are calculated 2θ angles for Bragg peaks.

(16). The scan conditions were angular range 8–70° (2θ), step size 0.02°, and counting for 17 s per step. The last refinement converged to $R_{wP} = 11.5\%$, $R_P = 8.8\%$, and $R_F = 3.3\%$. The atomic positions and the temperature factors needed to be refined to get the best possible agreement. The deviations with respect to the single-crystal structure were very small and hence, the atomic parameters (with larger errors) are not reported. The low-angle region of the refined powder pattern is shown in Fig. 6. It is worth emphasizing that the March–Dollase correction of the preferred orientation converged to a value that was 1.0 inside four times its standard deviation. So, the TASC method is very powerful to avoid the preferred orientation. Second, a very strong anisotropic peak broadening is observed along the [100] direction. This can be seen in the enlarged view of the refined powder diffraction pattern, Fig. 6. The anisotropic broadening is mainly Lorentzian and d^* dependent which means that broadening due to microstrains is prominent in the sample. This explains the difficulties in growing single crystals close to room temperature as these observed defects (probably due to slightly different water contents in the coherent diffraction domains) yield very poor quality and small single crystals at room temperature.

ACKNOWLEDGMENTS

The works in Málaga and Oviedo were supported by research grants FQM-113 (of Junta de Andalucía) and DGES (PB96-0556), respectively.

REFERENCES

1. A. Clearfield, *in* "Progress in Inorganic Chemistry" (K. D. Karlin, Ed.), Vol. 47, p. 371, Wiley, New York, 1998.
2. S. Drumel, V. Penicaud, D. Deniaud, and B. Bujoli, *Trends Inorg. Chem.* **4,** 13 (1996).
3. M. E. Thompson, *Chem. Mater.* **6,** 1168 (1994).
4. M. B. Dines, R. E. Cooksey, P. C. Griffith, and R. H. Lane, *Inorg. Chem.* **22,** 1003 (1983); G. Alberti, R. Costantino, F. Marmottini, and Z. P. Vivaniv, *Angew. Chem. Int. Ed. Engl.* **32,** 1357 (1993); G. Alberti, F. Marmottini, S. Murcia-Mascaros, and R. Vivani, *Angew. Chem., Int. Ed. Engl.* **33,** 1594 (1994); D. M. Poojary, B. Zhang, P. Bellinghausen, and A. Clearfield, *Inorg. Chem.* **35,** 5254 (1996); D. M. Poojary, B. Zhang, P. Bellinghausen, and A. Clearfield, *Inorg. Chem.* **35,** 4942 (1996).
5. B. Bujoli, A. Courilleau, P. Palvadeau, and J. Rouxel, *Eur. J. Solid State Inorg. Chem.* **92,** 171 (1992); S. Drumel, M. Bujoli-Doueff, P. Janvier, and B. Bujoli, *New J. Chem.* **19,** 239 (1995); S. Drumel, P. Janvier, P. Barboux, M. Bujoli-Doeuff, and B. Bujoli, *Inorg. Chem.* **34,** 148 (1995); P. Janvier, S. Drumel, P. Piffard, and B. Bujoli, *C. R. Acad. Sci. Paris, Ser. II* **320,** 29 (1995).
6. R. LaDuca, D. Rose, J. R. D. DeBord, R. C. Haushalter, C. J. O'Connor, and J. Zubieta, *J. Solid State Chem.* **123,** 408–412 (1996) and references therein.
7. M. I. Khan, Y. S. Lee, C. J. O'Connor, R. C. Haushalter, and J. Zubieta, *J. Am. Chem. Soc.* **116,** 4525 (1994).
8. A. Cabeza, M. A. G. Aranda, and S. Bruque, *J. Mater. Chem.* **9,** 571 (1999).
9. M. S. Lehman and F. K. Larsen, *Acta Crystallogr. A* **30,** 580 (1974).
10. D. F. Grant and E. J. Gabe, *J. Appl. Crystallogr.* **11,** 114 (1978).
11. G. M. Sheldrick, SHELXS86, *in* "Crystallographic Computing 3" (G. M. Sheldrick, C. Kruger, and R. Goddard, Eds.), Clarendon, Oxford, 1985.

12. P. T. Beurskens, G. Admiraal, G. Beurskens, W. P. Bosman, S. García-Granda, R. O. Gould, J. M. M. Smits, and C. Smykalla, "The DIRDIF program system. Technical Report of The Crystallography Laboratory," University of Nijmejen, The Netherlands, 1992.
13. G. M Sheldrick, SHELXL93, *in* "Crystallographic Computing 6" (H. D. Flack, P. Parkanyi, and K. Simon, Eds.), IUCr/Oxford Univ. Press, London, 1993.
14. "International Tables for X-Ray Crystallography," Vol. IV, Kynoch Press, Birmingham, (present distributor: Kluwer Academic Publishers, Dordrecht), 1974.
15. M. Nardelli, *Comput. Chem.* **7,** 95 (1983).
16. A. Cabeza, E. R. Losilla, H. S. Martínez-Tapia, S. Bruque, and M. A. G. Aranda, *Adv. X-ray Anal*. (1998) in press.
17. P. E. Werner, L. Eriksson, and M. Westdahl, *J. Appl. Crystallogr*. **18,** 367–370 (1985).
18. P. M. Wolff, *J. Appl. Crystallogr*. **1,** 108–113 (1968).
19. H. M. Rietveld, *J. Appl. Crystallogr*. **2,** 65 (1969).
20. A. C. Larson and R. B. von Dreele, Los Alamos National Lab. Rep. No. LA-UR-86-748, 1994 (Program version: PC).